

11-02
1

NASA Technical Memorandum 107581

P. 13

NACA0012 BENCHMARK MODEL EXPERIMENTAL FLUTTER RESULTS WITH UNSTEADY PRESSURE DISTRIBUTIONS

**José A. Rivera, Jr., Bryan E. Dansberry, Robert M. Bennett,
Michael H. Durham, and Walter A. Silva**

March 1992



National Aeronautics and
Space Administration

Langley Research Center
Hampton, Virginia 23665

(NASA-TM-107581) NACA0012 BENCHMARK MODEL
EXPERIMENTAL FLUTTER RESULTS WITH UNSTEADY
PRESSURE DISTRIBUTIONS (NASA) 13 pCSCL 01A

N92-22507

Unclass

G3/02 0085184

NACA 0012 BENCHMARK MODEL EXPERIMENTAL FLUTTER RESULTS WITH UNSTEADY PRESSURE DISTRIBUTIONS

José A. Rivera, Jr., Bryan E. Dansberry, Robert M. Bennett,
Michael H. Durham, and Walter A. Silva

NASA Langley Research Center
Hampton, VA 23665-5225

Abstract

The Structural Dynamics Division at NASA Langley Research Center has started a wind tunnel activity referred to as the Benchmark Models Program. The primary objective of the program is to acquire measured dynamic instability and corresponding pressure data that will be useful for developing and evaluating aeroelastic type CFD codes currently in use or under development. The program is a multi-year activity that will involve testing of several different models to investigate various aeroelastic phenomena. This paper describes results obtained from a second wind tunnel test of the first model in the Benchmark Models Program. This first model consisted of a rigid semispan wing having a rectangular planform and a NACA 0012 airfoil shape which was mounted on a flexible two degree-of-freedom mount system. Experimental flutter boundaries and corresponding unsteady pressure distribution data acquired over two model chords located at the 60 and 95-percent span stations are presented.

Introduction

The development of unsteady aeroelastic computational fluid dynamic (CFD) codes requires experimental data to validate computed results and/or for use as a guide for modification of analyses methods. The Benchmark Models Program¹ was

initiated by the Structural Dynamics Division at NASA Langley Research Center to provide such experimental data and to aid in understanding the flow phenomena associated with unusual aeroelastic phenomena.

The Benchmark Models Program (BMP) has identified several aerodynamic configurations to be tested in the NASA Langley Transonic Dynamics Tunnel (TDT). Some configurations are models for testing on a flexible mount system, referred to as the Pitch and Plunge Apparatus (PAPA). The NACA 0012 airfoil rectangular wing is the first of these BMP PAPA mounted models. To date, two comprehensive wind tunnel tests have been conducted for this model. During the first wind-tunnel test, flutter boundaries were defined and wing surface pressure measurements were obtained for a partial set of pressure transducers at the 60-percent span station. Preliminary results from this test are presented in reference 2. These results were used primarily as a guide for defining the scope of the second test. The second wind-tunnel test of this model was conducted to determine the flutter boundaries while simultaneously taking surface pressure measurements at most flutter conditions. For the second test, additional pressure transducers were installed on the wing to give more wing surface pressure measurements at both the 60-percent and 95-percent span stations. These flutter boundaries and the wing surface pressure data measured for the conventional flutter boundary are presented in reference 3 in tabular format. Reference 3 also contains an extensive set of

wing surface pressure measurements obtained with the model support system rigidized.

This paper focuses on the flutter and pressure data available from reference 3 to highlight Mach number effects on the flutter boundary and to correlate the measured pressure distributions with the conventional flutter boundary at transonic Mach numbers. The conventional flutter boundary, a plunge instability region near $M=0.90$, and the stall flutter boundary at $M=0.78$ are presented. In addition unsteady wing surface pressure measurements acquired during conventional flutter are presented in coefficient form and discussed.

Nomenclature

a	Speed of sound, ft/sec
C_p	Mean pressure coefficient during flutter
c	Wing streamwise local chord length, 16-inches
f	Frequency, Hz
f_2	Wind-off pitch frequency, 5.20 Hz
f_f	Flutter frequency, Hz
f_f/f_2	Flutter frequency ratio
g	Structural damping
k	Reduced frequency, $k=(c/2)\omega/V$
l	Wing spanwise length, 32 inches
L.E.	Leading edge
m	Calculated moving mass of wing/PAPA mechanism, 5.966 slugs
M	Free-stream Mach number
Phase	Phase angle referenced to pitch displacement, degrees
q	Free-stream dynamic pressure, psf
R_n	Reynolds number based on chord length
T.E.	Trailing edge
V	Free-stream velocity, ft/sec
V_I	Flutter speed index, $V_I=V/(c/2)\omega\sqrt{\mu}$
x	Distance from wing leading edge, inches
x/c	Fraction of local chord
z	Vertical (plunge) displacement, inches
α	Wing angle of attack (also alpha), degrees
θ	Pitch displacement, degrees
μ	Mass ratio, $\mu= m/\pi\rho l(c^2/4)$
ρ	Density, slugs/ft ³
ω	Circular frequency, rad/sec

Apparatus

Wind Tunnel

The wind-tunnel tests were conducted in the Langley Transonic Dynamics Tunnel (TDT).⁴ The TDT is a continuous flow, single return wind tunnel with a 16-foot square test section (with cropped corners) having slots in all four walls. It is capable of

operating at Mach numbers up to 1.2 and at stagnation pressures from near vacuum to atmospheric. The tunnel is equipped with four quick-opening bypass valves which can be used to rapidly reduce test-section dynamic pressure and Mach number when an instability occurs. Although either air or a heavy gas can be used as a test medium, only air was used for the present tests.

Model

The model is a semispan rigid wing mounted on a flexible mount system referred to as the Pitch and Plunge Apparatus (PAPA).^{5,6} A photograph of the model mounted in the TDT test section is shown in figure 1. A planform view of the model is shown in figure 2. The model has a NACA 0012 airfoil section and a rectangular planform with a span of 32 inches and a chord of 16 inches. The mount system is attached to a turntable which provides for angle-of-attack variation. Transition strips made up of No. 30 carborundum grit were applied to the model approximately one inch back from the leading edge (approximately 6-percent chord) on both the upper and lower surfaces.

The model was designed to allow installation of 80 in-situ pressure transducers for measurement of unsteady wing surface pressures. These pressure transducers were referenced to wind-tunnel static pressure. Forty of the transducers are located at the 60-percent span station, and forty at the 95-percent span station. The span locations for these pressure measurements are indicated in figure 2. The physical locations of orifices and corresponding pressure transducers on the airfoil cross section are available in reference 3 and illustrated in figure 3.

Details of the model construction can be seen in the photographs of figure 4. The lower photograph shows that the model was fabricated in three sections. Each section was machined from solid aluminum stock. The sections were bolted together after the pressure transducers, reference pressure tubes, and wiring were installed. In the upper left photograph is an expanded view of a portion of the mid section which shows holes drilled in the edge of the section. These holes were used for insertion of the pressure transducers. Two pressure transducers are shown next to the model. One of the pressure transducers is shown mounted in a brass tube. The brass tube is used to protect the transducer when it is inserted and removed from the model. The associated orifice holes for the pressure transducers are located about one inch from the inboard edge of the mid section and tip section. When the pressure transducers and sleeves are inserted, the measurement face of the pressure transducer is within 0.2 inch of the orifice location on

the wing surface where the pressure measurement is being made. Exceptions are the trailing edge pressure transducers which are approximately 0.7 inch from the orifice location.

There are four accelerometers in the model, one near each corner, used to assist in identifying model dynamic characteristics during testing. These accelerometers are mounted in pockets, one of which is shown in the photograph in the upper right of figure 4.

Mount System

The model mounting system is composed of two basic parts. They include a flexible support and a large splitter plate. The model is mounted outboard of the splitter plate.

The flexible support, which allows pitch and plunge motion of the model, is located behind the splitter plate. A description of the flexible mount system, referred to as the PAPA (Pitch and Plunge Apparatus),^{5,6} is presented in figures 5, 6, and 7. Figure 5 is a photograph which shows a moving plate supported out from the tunnel wall by a system of four rods and a centerline flat plate drag strut all with fixed-fixed end conditions. At the tunnel wall the rods and drag strut are attached to a mounting plate attached to a turntable so that the model angle of attack can be varied.

The rods and flat plate drag strut provide linearly constrained motion so that the model can oscillate sinusoidally in pitch and plunge. The oscillations are functions of the stiffness of the rods, the mass properties of the moving apparatus, and the aerodynamic forces on the model. The structural properties of this simple mount system can be well defined mathematically and can be easily measured for flutter calculations. This makes the PAPA mount system a valuable tool for obtaining experimental model flutter data for correlation with analysis because disagreement between theory and experiment can be primarily attributed to aerodynamics. The PAPA is instrumented with two strain gage bridges oriented to measure bending and torsional moments from which wing model instantaneous plunge position and pitch angle can be obtained. These are located on the flat plate drag strut near the mounting plate.

The PAPA splitter plate, shown in figure 6, is suspended out from the test-section wall by struts which are about 40 inches long. The splitter plate is 12 feet long and 10 feet high. The centerline of the model and the PAPA support system is 7 feet rearward from the leading edge of the splitter plate. The PAPA mount system rods and drag strut are enclosed in a fairing behind the splitter plate. The

wing model and end plate are the only parts of the apparatus that are exposed to the flow in the test section. The splitter plate serves to separate flow over the model from flow around the mount system fairing which is located between the splitter plate and the test section wall.

A top view sketch which shows how the wing model, the PAPA apparatus, the splitter plate and other components fit together is presented as figure 7. The model is attached to a short pedestal or spacer which protrudes through the opening in the splitter plate, all of which attaches to the moving plate. The moving plate has provisions for the addition of ballast weights (indicated in figure 7) to adjust the mount system structural dynamic characteristics. The opening in the splitter plate is covered by a thin circular end plate attached to the root section of the model to prevent flow through the splitter plate. The circular end plate has a diameter equal to the model chord length. The circular plate can be seen in the photograph of figure 6. The gap between the end plate and the splitter plate was less than one-tenth of an inch, but sufficient so that the end plate did not rub against the splitter plate.

Structural Dynamic Characteristics

The first two wind-off natural modes of vibration for the NACA 0012 model/PAPA mount system assembly are the wing-model rigid-body plunge and rigid-body pitch modes respectively. Inertia coupling between these two modes was eliminated by positioning ballast weights on the PAPA system moving plate so that the system center of gravity was on the PAPA elastic axis (centerline). Therefore the rigid-body plunge mode consists only of vertical translation of the wing model and the rigid-body pitch mode consists only of rotation of the wing model about the mid-chord. The measured frequencies, damping and stiffnesses for these two modes are presented in table 1. Modal displacements for corresponding, unit-generalized-masses are presented in table 2.

Data Acquisition and Reduction

Wing model and mount system transducer time history data were acquired at the conventional flutter boundary test conditions with the TDT data acquisition system. The data were acquired simultaneously (not multiplexed) for all transducers at a rate of 100 samples per second for 40 seconds and recorded in digital form on disk.

For each differential pressure transducer (the pressure transducers were referenced to wind-tunnel

static pressure) the mean pressure was calculated using all 4000 samples of data. This mean pressure value was divided by the dynamic pressure (q) at the flutter condition to form a mean pressure coefficient C_p .

A discrete Fourier analysis, at the flutter frequency, was used to determine the magnitude and phase of the oscillating pressure distribution during flutter. The magnitudes of the pressure distribution were normalized by the magnitude of the oscillating pitch angle, and the phase angles are relative to the pitch motion. A phase angle is positive when a pressure transducer oscillatory signal leads the wing pitch motion.

For the conventional flutter boundary measurements, the turntable pitch angle was set at zero degrees and determined by a servo accelerometer. The bending and torsion strain gage bridges on the PAPA support system were calibrated to obtain plunge position and pitch angle of the wing model relative to the turntable. At the flutter conditions the plunge and pitch motion of the wing model, and the flutter frequency, were determined from these strain gage bridge measurements.

Results and Discussion

Instability Boundaries

Conventional flutter, plunge instability, and stall flutter boundaries were defined during testing. These boundaries are similar to those encountered during the first test as described in reference 2. As mentioned previously, results presented herein are from the second test only.

Conventional flutter.- The flutter boundary for zero degrees angle of attack, is shown in figure 8 as flutter dynamic pressure versus Mach number. The conventional flutter data is represented by the square symbols. The model is stable below the boundary and is unstable above the boundary. An unusual trend of an increase in flutter dynamic pressure with Mach number is shown. This is probably a result of the elastic axis of the wing/mount system being located at the wing mid-chord. There is a small transonic dip near $M=0.77$ followed by a sharp upward turn of the boundary near $M=0.80$. The flutter boundary is well defined with a large number of flutter points and relatively small scatter. A tabulation of the test conditions and flutter parameters for each test point on the conventional flutter boundary are presented in table 3. Also included in table 3 are the magnitude and phase of the pitch and plunge displacement during flutter, θ and z respectively.

Plunge instability.- A plunge instability region is shown also in figure 8. This plunge instability is represented by the circular symbols and the cross hatched area which covers a narrow transonic Mach number range from about $M=0.88$ to 0.95 . As implied, the flutter motion consisted of primarily the plunge mode. A tabulation of the test conditions for the test points identifying the plunge instability region are presented in table 4. At dynamic pressures below 140 psf, testing was able to proceed through the instability region so that both the lower Mach number side of the instability boundary and the upper Mach number side of the instability boundary could be defined. At dynamic pressures at or above 140 psf, testing was terminated because the model motions were so large that only the low Mach number side of the instability boundary could be identified. Flow visualization using tufts indicated strong shock-induced separation for this Mach number range. An instability having similar characteristics was reported in reference 7 for a transport type wing.

Stall flutter.- Additional flutter results are presented in figure 9 for a Mach number of 0.78 which demonstrates the effects of angle-of-attack on the dynamic pressure at which flutter was encountered. The results show that the dynamic pressure increases by a small amount as angle-of-attack is increased from zero up to about 4 degrees. At angles-of-attack above 4 degrees there is a rapid drop in the dynamic pressure at which flutter was encountered. This rapid decrease in the boundary above 4 degrees is associated with wing stall conditions during a portion of the pitch oscillation cycle.

Pressure measurements at the conventional flutter boundary

Wing surface pressures were measured during most of the flutter points shown previously. At this time, only the pressure data for the conventional flutter boundary have been processed and made available in tabular form in reference 3. These measured pressure data for selected Mach numbers including the transonic range are presented and discussed herein.

Mean pressure measurements.- Plots showing the mean values of the pressure coefficient (C_p) for the upper surface as a function of chord position x/c for the 60-percent and 95-percent span stations are presented in figure 10 for $M=0.30, 0.67, 0.71, 0.77, 0.80, 0.82$. Each line connects the C_p values at one Mach number and is representative of the mean pressure distribution during flutter. For ease of interpretation, data for $M=0.30, 0.67, 0.71, 0.77$ are

presented at the top of the figure. These data were acquired during flutter at conditions defining the subsonic portion of the boundary and the transonic dip (indicated in figure 8). The data for $M=0.77, 0.80, 0.82$ are presented at the bottom. These were acquired at conditions defining the sharp upward turn of the boundary. The data for $M=0.77$ is presented in both locations to serve as a reference during comparisons. No lower surface C_p values are presented because the airfoil is symmetric and the mean angle of attack was essentially zero.

The transition strip was located on the wing at approximately the 6-percent chord. The pressures between 5-percent and 10-percent chord in the area of the transition strip appear to be irregular. This may be a local effect of the grit but requires further study. There are also some point to point variations in the measured pressures at the higher Mach numbers that also warrant further study.

At the top of figure 10 the effects on C_p mean as Mach number increases from 0.30 to 0.77 are shown. From $M=0.30$ to 0.67 the effects are small (recalling figure 8, Mach 0.30 and 0.67 correspond to the subsonic portion of the flutter boundary). The largest value of C_p increases a small amount with Mach number at both span stations, and the position on the chord (x/c) where the largest value occurs moves aft from about 10-percent to 15-percent chord at the 60-percent span. No significant movement from $x/c=.10$ is noted at the 95-percent span. As Mach number increases from $M=0.67$ to 0.77 the effects on the pressures are more noticeable. At $M=0.77$ the largest value of C_p aft of the transition strip has increased to -0.7 at the 60-percent span and the x/c location has moved aft to 20-percent chord. The drop in C_p aft of $x/c=0.20$, (when compared to the lower Mach numbers) indicates the presence of a shock. At the 95-percent span the largest C_p aft of the transition strip has increased to -0.5 and the location has moved to 15-percent chord ($x/c=0.15$).

At the bottom of figure 10 the effects on C_p mean as Mach number increases from 0.77 to 0.82 are shown. Recalling figure 8, between $M=0.77$ and 0.82 the flutter boundary turns upward and rises rapidly. At these Mach numbers the mean values of pressure coefficient (shown at the bottom of figure 10) indicate that the shock strengthens and moves aft to near the 40-percent chord at the 60-percent span. At the 95-percent span a weak shock appears near the 20-percent chord at $M=0.80$ and 0.82.

Unsteady pressure measurements. The magnitude of the unsteady pressure coefficients (C_p Magnitude) and the phase relative to the pitch displacement of the wing model, during flutter, were obtained from a

discrete Fourier analysis at the flutter frequency. C_p Magnitude versus x/c plots are presented in figure 11 for $M=0.30, 0.67, 0.71, 0.77, 0.80, 0.82$. For ease of interpretation, data for $M=0.30, 0.67, 0.71, 0.77$ are presented at the top of the figure and the data for $M=0.77, 0.80, 0.82$ are presented at the bottom. The data for $M=0.77$ are presented in both locations to serve as a reference during comparisons. Data are presented on the left for the 60-percent span station and on the right for the 95-percent span station. The lower surface C_p Magnitude and phase values are not presented. The upper and lower surface measurements were in very good agreement and indicated the same trends as they should for zero angle-of-attack.

At $M=0.77$ and the higher Mach numbers, the pressures immediately downstream of the transition strip (near 6-percent chord) are anomalous on both chords. The effect appears to be localized and due to the transition strip but requires further study.

At the top of figure 11 the effects on C_p Magnitude as Mach number increases from 0.30 to 0.77 are shown. At Mach numbers between $M=0.30$ and 0.71 the unsteady pressure coefficient magnitude for both the 60-percent and 95-percent span surface measurements are typical subsonic distributions with a peak dynamic loading near the wing leading edge followed by a decrease at locations further aft. The data appear smooth with little scatter. As Mach number increases to $M=0.77$ and above, the results show two peaks in the pressure data. The first peak, located near the 6-percent chord, appears to be a result of the transition strip on the wing model. At $M=0.77$, the second peak loading is near the shock wave location at the 25-percent chord as would be expected. As Mach number increases to $M=0.82$ (bottom of figure 11), the location on the chord at which this peak loading occurs moves aft to 45-percent chord at the 60-percent span station, and to 30-percent chord at the 95-percent span station. Recalling figure 8, these Mach numbers ($M=0.77$ to 0.82) correspond to points on the boundary defining the sharp upward turn in flutter dynamic pressure.

Figure 12 shows phase of C_p relative to pitch displacement of the wing model during flutter. Data are presented on the left for the 60-percent span station and on the right for the 95-percent span station. At subsonic Mach numbers a phase shift occurs near the trailing edge ($x/c=0.80$). As Mach number increases to $M=0.77$ the position on the chord of this phase shift progresses forward gradually to about $x/c=0.65$. As Mach number increases to $M=0.80$ the phase shift occurs at the most forward location near $x/c=0.40$, then reverses and moves aft to about $x/c=0.50$ at $M=0.82$.

Concluding Remarks

The Benchmark Models Program (BMP) has been initiated with the primary objective of obtaining data for aeroelastic CFD code development, evaluation, and validation. The first BMP model consisted of a rigid semispan wing having a rectangular planform and a NACA 0012 airfoil shape. This model was mounted on a flexible two degree-of-freedom mount system. Tests on the first BMP model have been conducted in the NASA Langley Transonic Dynamics Tunnel to investigate instability boundaries while simultaneously taking surface pressure measurements at most instability conditions. Several different types of dynamic instability were investigated. They included conventional flutter, a plunge instability, and stall flutter. This paper focuses on the flutter and pressure data available from these test results. The conventional flutter boundary, the plunge instability region, and the stall flutter boundary at Mach=0.78 are presented. In addition, Mach number effects on the conventional flutter boundary are correlated with the measured pressure distributions at the flutter condition. The results are summarized as follows:

1. The conventional flutter boundary is characterized by an unusual trend of an increase in flutter dynamic pressure with Mach number. There is a small transonic dip near Mach=0.77 with a sharp upward turn of the boundary near Mach=0.80.

2. A plunge instability region was observed over a narrow Mach number range from about M=0.88 to M=0.95. The wing flutter motion was observed to be primarily that of the plunge mode.

3. The stall flutter boundary at M=0.78 exhibits a small increase in flutter dynamic pressure as angle-of-attack is increased up to about 4 degrees. At angles-of-attack above 4 degrees there is a rapid drop in the dynamic pressure at which flutter is encountered.

4. The unsteady surface pressure measurements at the 60-percent and 95-percent span stations obtained at the conventional flutter boundary indicate the following:

- a. At Mach numbers between M=0.30 and M=0.71 the unsteady surface pressure measurements show typical subsonic distributions with peak dynamic loading near the wing leading edge followed by a decrease at locations further aft.
- b. Between M=0.71 and M=0.77 the measured pressures at the 60-percent span indicate the formation of a shock near the 25-percent chord. As Mach number increases to M=0.82 this shock

strengthens and moves aft to approximately the 45-percent chord.

- c. At M=0.80 and M=0.82 the pressure measurements at the 95-percent span indicate a weak shock at approximately the 20-percent chord. The peak dynamic loading due to this shock moves aft from approximately the 20-percent chord to approximately the 30-percent chord as Mach number increases from M=0.80 to M=0.82.

Current activities include further evaluation of the surface pressure measurements. Early release of these experimental results is intended to help in the development and validation of aeroelastic CFD codes.

References

1. Bennett, Robert M.; Eckstrom, Clinton V.; Rivera, José A., Jr.; Dansberry, Bryan E.; Farmer, Moses G.; and Durham, Michael H.: The Benchmark Aeroelastic Models Program - Description and Highlights of Initial Results. Presented at the AGARD Structures and Materials Panel Specialists' Meeting on TRANSONIC UNSTEADY AERODYNAMICS AND AEROELASTICITY. San Diego, California. October 9-11, 1991. Paper No. 25, also available as NASA TM-104180, 1991.
2. Rivera, José A., Jr.; Dansberry, Bryan E.; Farmer, Moses G.; Eckstrom, Clinton V.; Seidel, David A.; and Bennett, Robert M.: Experimental Flutter Boundaries with Unsteady Pressure Distributions for the NACA 0012 Benchmark Model. AIAA Paper No. 91-1010, 1991. Also NASA TM-104072, 1991.
3. Rivera, José A., Jr.; Dansberry, Bryan E.; Durham, Michael H.; Bennett, Robert M.; and Silva, Walter A.: Pressure Measurements on a Rectangular Wing with a NACA 0012 Airfoil during Conventional Flutter. NASA TM 104211, 1992.
4. Reed, Wilmer H.: Aeroelasticity Matters: Some Reflections of Two Decades of Testing in the NASA Langley Transonic Dynamics Tunnel. NASA TM-83210, 1981.
5. Farmer, Moses G.: A Two-Degree-of-Freedom Flutter Mount System with Low Damping for Testing Rigid Wings at Different Angles of Attack. NASA TM-83302, 1982.
6. Farmer, Moses G.: Model Mount System for Testing Flutter. U.S. Patent Number 4,475,385, Oct. 9, 1984.
7. Eckstrom, Clinton V.; Seidel, David A.; and Sandford, Maynard C.: Unsteady Pressure and Structural Response Measurements on an Elastic Supercritical Wing. Journal of Aircraft, Vol. 27, No. 6, June 1990.

Table 1. Measured frequency, damping, and stiffness.

Mode	Frequency (Hz)	Structural Damping, g	Measured Stiffness
Plunge	3.36	0.0024	2659 lbs/ft
Pitch	5.20	0.0024	2897 ft-lbs/rad

Table 2. Modal displacements and generalized mass.

Mode	Modal Displacement		Generalized Mass / Inertia
	leading edge	trailing edge	
Plunge	+0.4094 ft	+0.4094 ft	1.0 slug
Pitch	+0.4047 ft	-0.4047 ft	1.0 slug-ft ²

Table 3. Experimental results for the conventional flutter boundary.

Mach	q (lb/ft ²)	a (ft/sec)	V (ft/sec)	ρ (slugs/ft ³)	Rn x10 ⁻⁶	μ	V _I	f _r (Hz)	f _r /f ₂	k	z		θ	
											Mag (in)	Phase (deg)	Mag (deg)	Phase (deg)
* 0.30	131.7	1127.2	338.2	0.002303	2.736	696	0.563	4.56	0.877	0.0565	0.27	-175.5	1.63	0.
0.39	137.2	1132.3	441.6	0.001407	2.168	1139	0.574	4.51	0.867	0.0428	0.35	-176.2	1.93	0.
0.45	137.7	1129.5	508.3	0.001066	1.897	1503	0.575	4.47	0.860	0.0368	0.23	-176.7	1.22	0.
0.51	141.9	1121.6	572.0	0.000867	1.755	1848	0.584	4.43	0.852	0.0324	0.32	-177.0	1.49	0.
0.61	144.6	1108.8	676.4	0.000632	1.540	2535	0.590	4.34	0.835	0.0269	0.25	-177.3	1.01	0.
* 0.67	146.5	1096.0	734.3	0.000543	1.463	2951	0.593	4.28	0.823	0.0244	0.34	-177.1	1.22	0.
* 0.71	146.9	1106.6	785.7	0.000476	1.316	3366	0.594	4.25	0.817	0.0227	0.26	-177.2	0.89	0.
* 0.77	144.2	1097.1	844.8	0.000404	1.251	3966	0.589	4.13	0.794	0.0205	0.36	-177.1	0.99	0.
* 0.80	147.2	1109.1	887.3	0.000374	1.196	4284	0.595	4.09	0.787	0.0193	0.25	-177.4	0.60	0.
* 0.82	159.9	1111.6	911.5	0.000385	1.259	4162	0.620	4.07	0.783	0.0187	0.21	-176.5	0.42	0.

* Mach numbers at which measured pressures are discussed in this report.
 Tabulated pressures are available for all the above Mach numbers in reference 3.

Table 4. Experimental results for the plunge instability region.

Mach	q (lb/ft ²)	a (ft/sec)	V (ft/sec)	ρ (slugs/ft ³)	Rn x10 ⁻⁶	μ	V _I
0.88	142.2	1091.5	960.5	0.000308	1.093	5202	0.584
0.88	108.4	1090.0	959.2	0.000236	0.838	6789	0.511
0.89	69.9	1076.3	957.9	0.000152	0.550	10541	0.409
0.90	59.8	1068.3	961.5	0.000129	0.474	12421	0.379
0.93	76.6	1076.1	1000.8	0.000153	0.578	10473	0.429
0.93	88.9	1079.4	1003.8	0.000176	0.664	9104	0.462
0.95	122.4	1089.5	1035.0	0.000229	0.878	6997	0.543

ORIGINAL PAGE
BLACK AND WHITE PHOTOGRAPH



Figure 1. NACA 0012 airfoil model mounted in TDT.

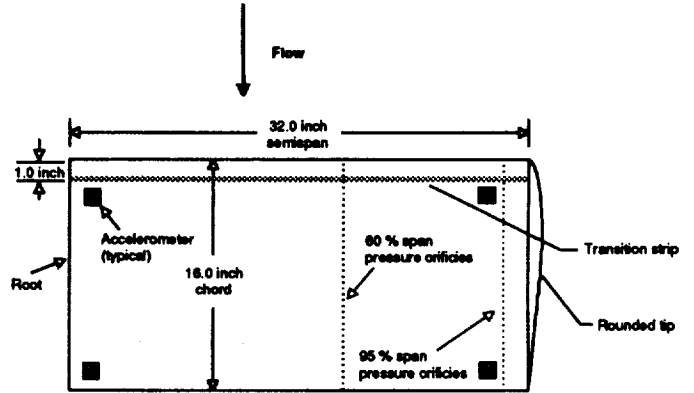


Figure 2. Wing model planform.

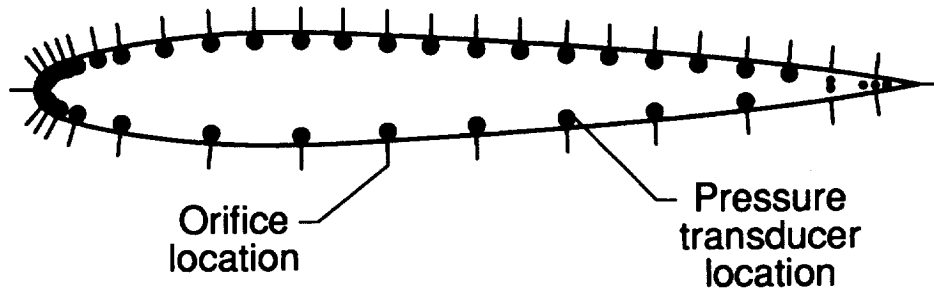


Figure 3. Orifice and pressure transducer locations at 60-percent and 95-percent span stations.

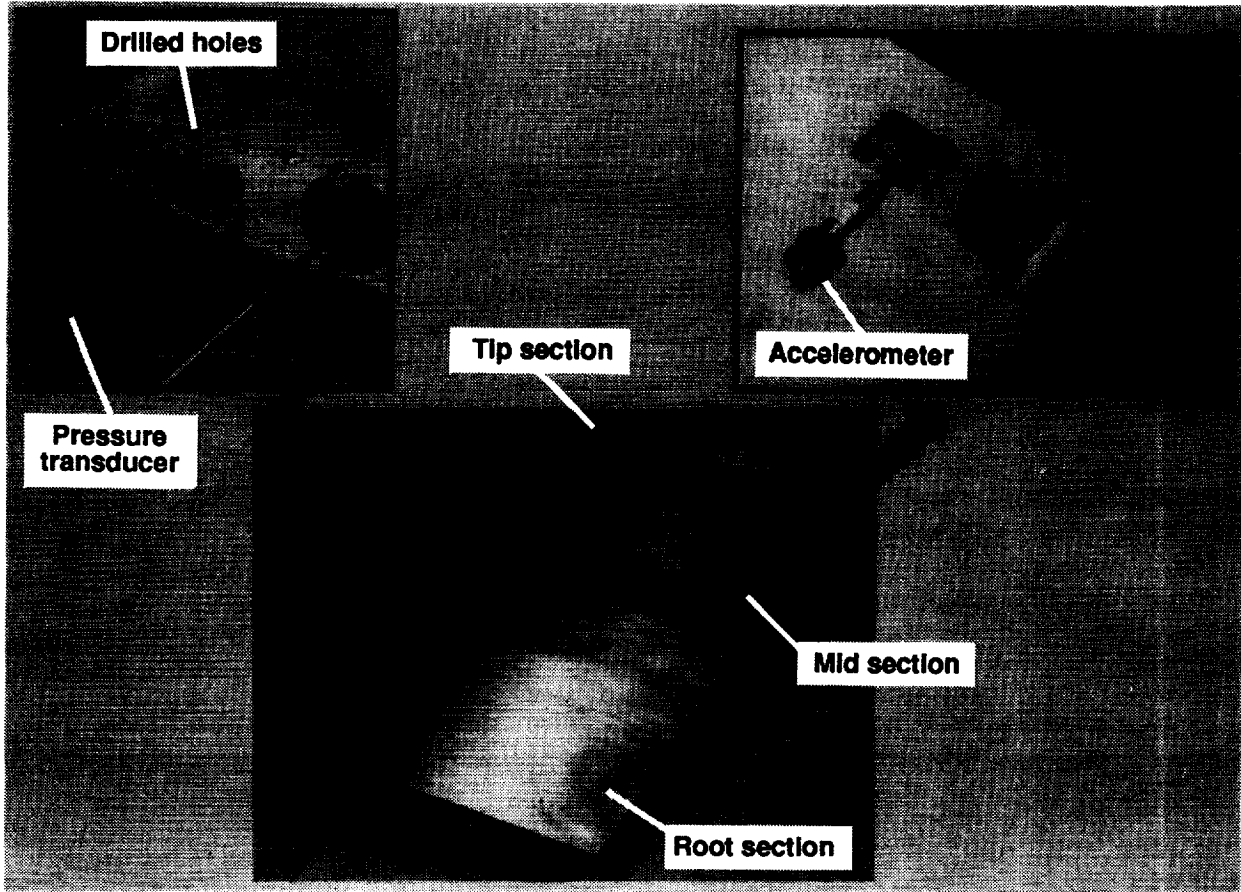


Figure 4. Model details.

ORIGINAL PAGE
BLACK AND WHITE PHOTOGRAPH

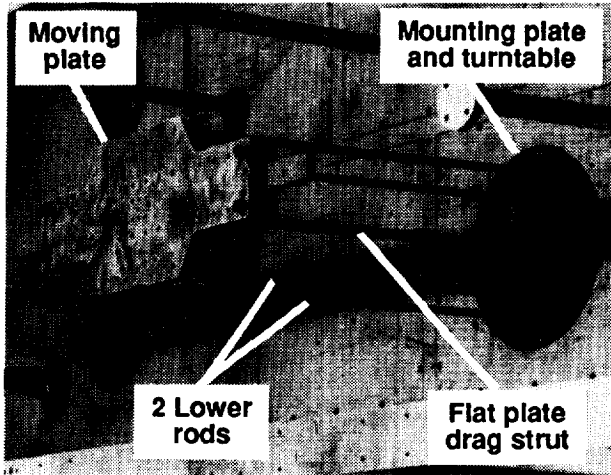


Figure 5. PAPA flexible mount.

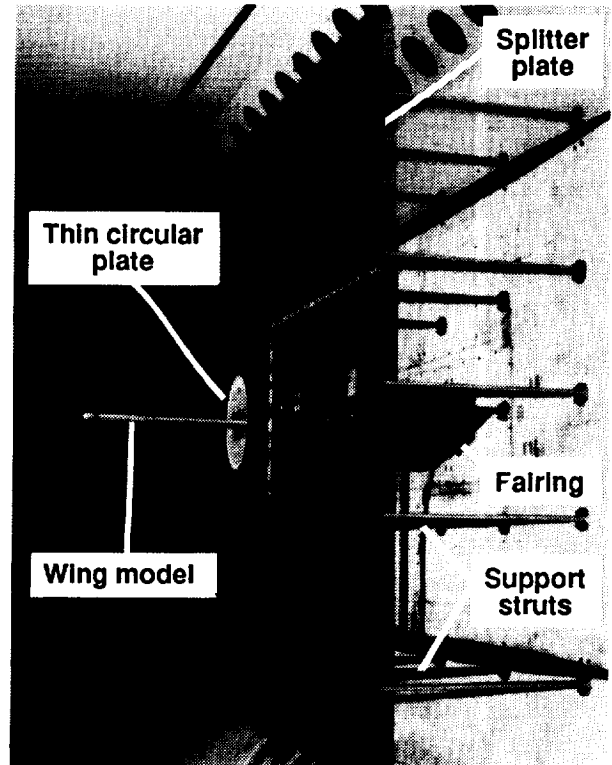


Figure 6. PAPA splitter plate.

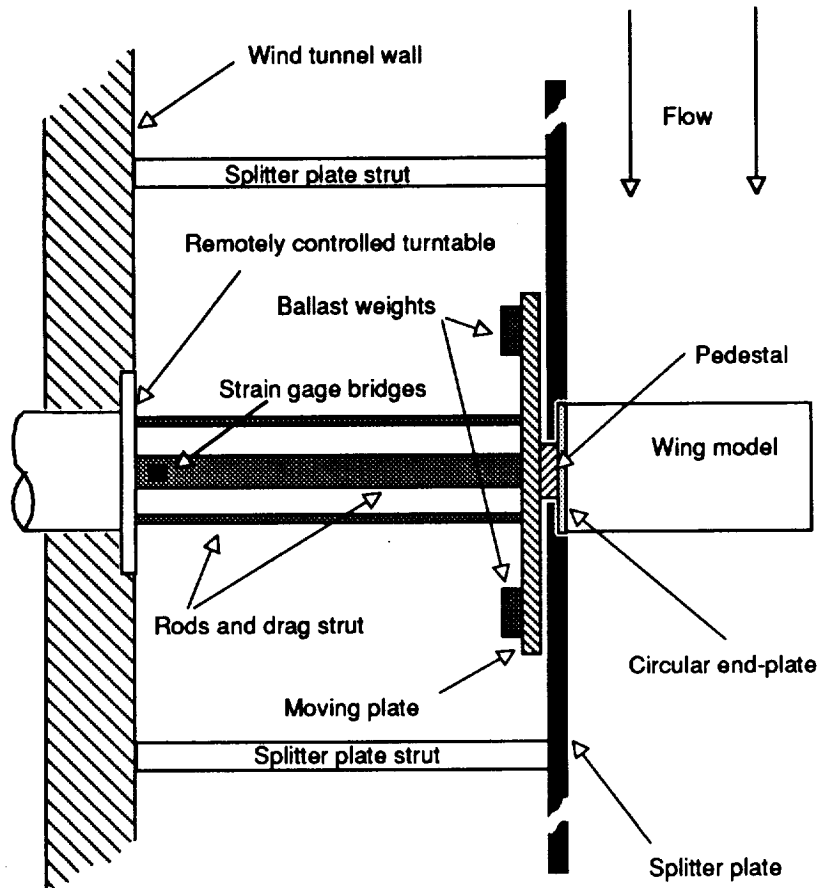


Figure 7. Top view sketch of the PAPA assembly (fairing over rods is not shown).

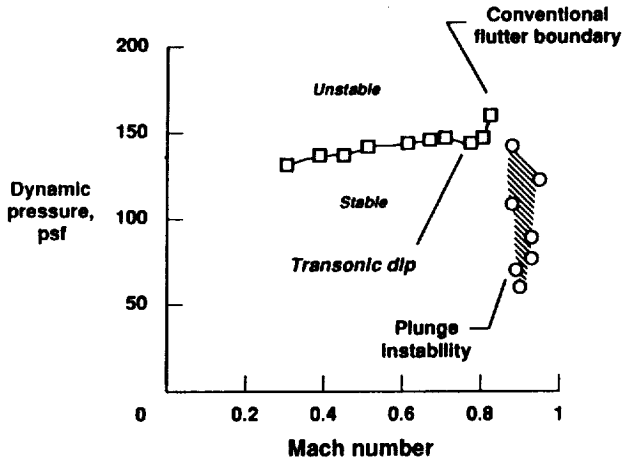


Figure 8. Conventional flutter boundary and transonic plunge instability region ($\alpha=0.0$ degrees).

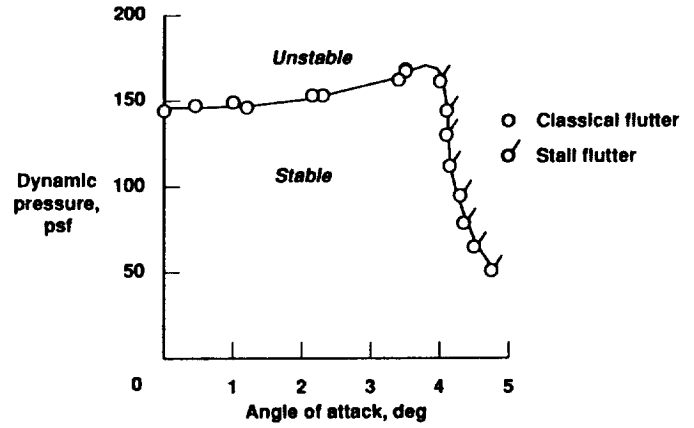


Figure 9. Stall flutter dynamic pressure versus angle-of-attack for $M=0.78$.

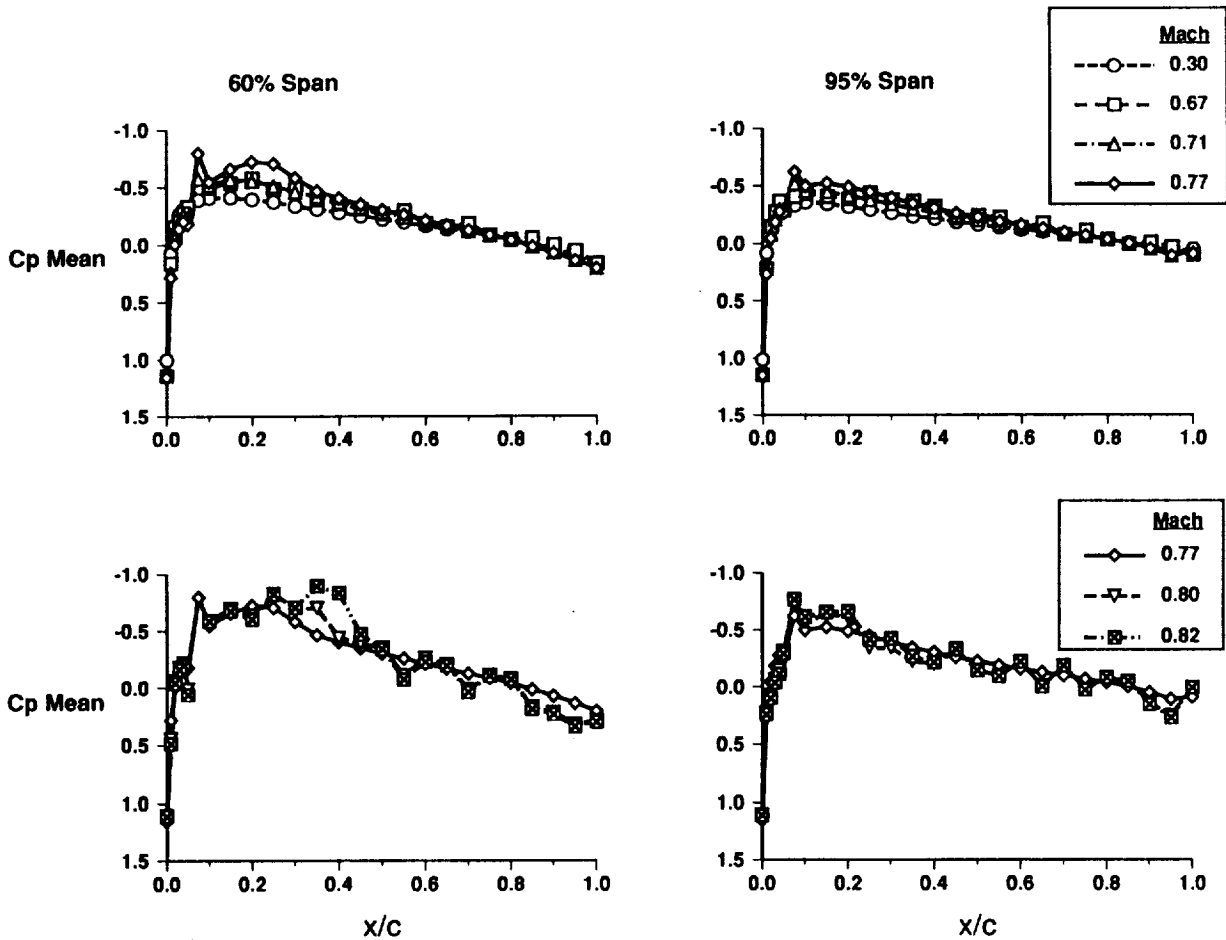


Figure 10. Upper surface mean pressure coefficient distribution during conventional flutter for several Mach numbers.

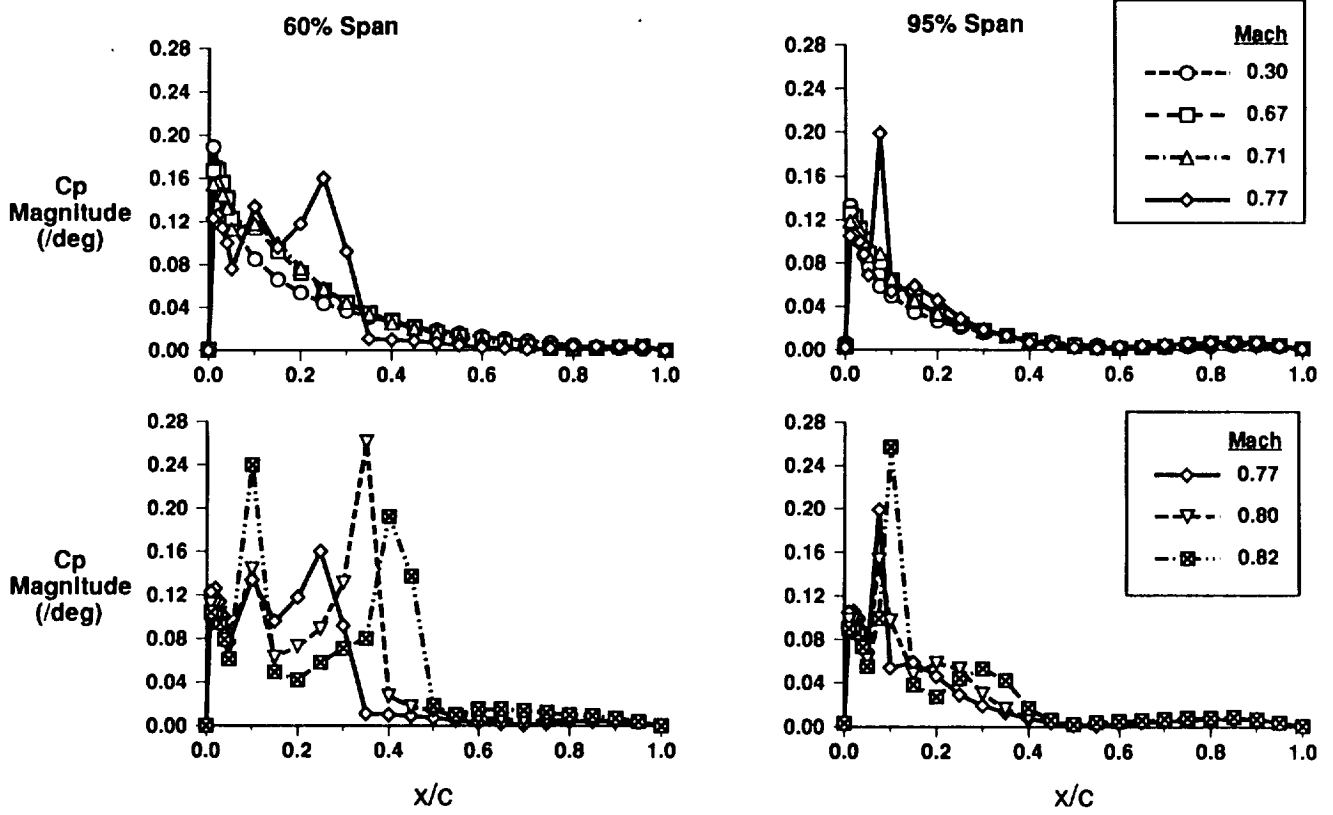


Figure 11. Magnitude of unsteady pressure coefficient distribution during conventional flutter for several Mach numbers.

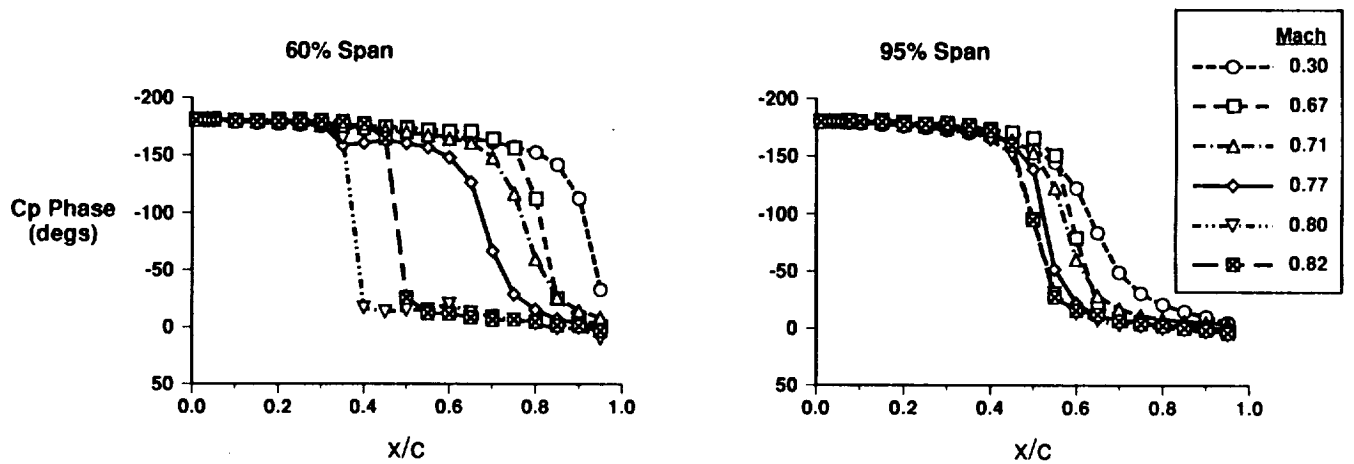


Figure 12. Phase of unsteady pressure coefficient distribution during conventional flutter for several Mach numbers.

REPORT DOCUMENTATION PAGE

Form Approved
OMB No. 0704-0188

Public reporting burden for this collection of information is estimated to average 1 hour per response, including the time for reviewing instructions, searching existing data sources, gathering and maintaining the data needed, and completing and reviewing the collection of information. Send comments regarding this burden estimate or any other aspect of this collection of information, including suggestions for reducing this burden, to Washington Headquarters Services, Directorate for Information Operations and Reports, 1215 Jefferson Davis Highway, Suite 1204, Arlington, VA 22202-4302, and to the Office of Management and Budget, Paperwork Reduction Project (0704-0188), Washington, DC 20503.

1. AGENCY USE ONLY (Leave blank)		2. REPORT DATE March 1992	3. REPORT TYPE AND DATES COVERED Technical Memorandum	
4. TITLE AND SUBTITLE NACA0012 BENCHMARK MODEL EXPERIMENTAL FLUTTER RESULTS WITH UNSTEADY PRESSURE DISTRIBUTIONS			5. FUNDING NUMBERS 505-63-50	
6. AUTHOR(S) J. A. Rivera, Jr., B. E. Dansberry, R. M. Bennett, M. H. Durham and W. A. Silva				
7. PERFORMING ORGANIZATION NAME(S) AND ADDRESS(ES) NASA Langley Research Center Hampton, VA 23665-5225			8. PERFORMING ORGANIZATION REPORT NUMBER	
9. SPONSORING/MONITORING AGENCY NAME(S) AND ADDRESS(ES) National Aeronautics and Space Administration Washington, DC 20546-0001			10. SPONSORING/MONITORING AGENCY REPORT NUMBER NASA TM-107581	
11. SUPPLEMENTARY NOTES This paper will be presented at the AIAA/ASME/ASCE/AHS/ASC 33rd Structures, Structural Dynamics, and Materials Conference, Dallas, Texas, April 13-15, 1992.				
12a. DISTRIBUTION / AVAILABILITY STATEMENT Unclassified - Unlimited Subject Category 02			12b. DISTRIBUTION CODE	
13. ABSTRACT (Maximum 200 words) The Structural Dynamics Division at NASA Langley Research Center has started a wind tunnel activity referred to as the Benchmark Models Program. The primary objective of the program is to acquire measured dynamic instability and corresponding pressure data that will be useful for developing and evaluating aeroelastic type CFD codes currently in use or under development. The program is a multi-year activity that will involve testing of several different models to investigate various aeroelastic phenomena. This paper describes results obtained from a second wind tunnel test of the first model in the Benchmark Models Program. This first model consisted of a rigid semispan wing having a rectangular planform and a NACA 0012 airfoil shape which was mounted on a flexible two degree-of-freedom mount system. Experimental flutter boundaries and corresponding unsteady pressure distribution data acquired over two model chords located at the 60 and 95-percent span stations are presented.				
14. SUBJECT TERMS Flutter Pressure Distributions			15. NUMBER OF PAGES 12	
			16. PRICE CODE A03	
17. SECURITY CLASSIFICATION OF REPORT Unclassified	18. SECURITY CLASSIFICATION OF THIS PAGE Unclassified	19. SECURITY CLASSIFICATION OF ABSTRACT Unclassified	20. LIMITATION OF ABSTRACT Unlimited	